Processing and Application of Ceramics 11 [3] (2017) 213–219
https://doi.org/10.2298/PAC1703213S

Performances of spin coated silver doped ZnO photoanode based dye sensitized solar cell

Amrik Singh[1,*], Devendra Mohan[2], Dharamvir Singh Ahlawat[1], Richa[3]

[1]*Material Science Lab., Department of Physics, Chaudhary Devi Lal University, Sirsa-125055 Haryana, India*
[2]*Laser Laboratory, Department of Applied Physics, Guru Jambheshwar University of Science & Technology, Hisar-125001, Haryana, India*
[3]*Research Scholar, Department of Physics, I.K. Gujral Punjab Technical University, Kapurthala-144601, Punjab, India*

Received 12 March 2017; Received in revised form 23 July 2017; Received in revised form 8 September 2017; Accepted 16 September 2017

Abstract

Dye sensitized solar cells (DSSCs) were fabricated using silver doped ZnO films deposited on ITO glass by spin coating method. The crystalline nature of ZnO films was analysed with XRD and SEM technique was used for morphological studies. The XRD pattern confirmed the presence of single phase hexagonal wurtzite ZnO structure, without the presence of secondary phase. The crystallite size of ZnO decreased from 31 nm to 25 nm with increase in doping to 1.5 mol% of silver. The UV-visible transmission of the prepared ZnO film was found to be 70–90% and it decreased with increase in doping to 0.5 mol% Ag and increased in the film doped with 1.5 mol% Ag. The band gap values of the ZnO films with 0, 0.5 and 1.5 mol% of silver, determined from Tauc plot, were 3.269, 3.235 and 3.257 eV, respectively. The absorbance peaks of the N719 dye loaded ZnO films were obtained at the wavelengths 310, 350 and 538 nm. The N719 dye loaded ZnO film doped with 0.5 mol% Ag has the highest absorbance in the visible region as compared to other two samples. The fill factor values of the pure and ZnO doped with 0.5 and 1.5 mol% Ag were 0.47, 0.48 and 0.42, respectively. The short circuit density values for ZnO, ZnO:Ag0.5% and ZnO:Ag1.5% were found to be 1.50, 1.55 and 1.15 A·m/cm^2, respectively. The calculated photon to electron efficiencies for the ZnO films with 0, 0.5 and 1.5 mol% of silver were 0.42%, 0.44% and 0.27%, respectively. Consequently future prospective of such type of dopants in ZnO film based dye sensitized solar cells seems to be bright.

Keywords: *Ag doped ZnO films, spin coating technique, solar cell, band gap, photovoltaic performances*

I. Introduction

Dye sensitized solar cells (DSSCs) have attracted considerable attention due to their low cost and relatively high photovoltaic performance [1–3].The DSSCs consist of photoanode, counterelectrode and electrolytes. The photoelectrode have semiconductor oxide layer like ZnO, TiO_2 and dye adsorbed into semiconductor oxide layer. On the other side, platinum or graphite acts as counterelectrode and iodine as redox couple electrolyte [4–8]. Transparent conducting oxide coated glass like ITO has been the main choice for the substrate material for the DSSC, due to its excellent optical, electrical and encapsulation barrier properties. As incident photons are absorbed by dye molecules, electrons are being injected from their excited states into the conduction band of the TiO_2/ZnO nanoparticles and the dye molecule gets oxidized. Oxidized dye molecules are reduced by a redox electrolyte, which transports the positive charges by diffusion to a counterelectrode [9–13]. Efficient electron injection from excited state of the dye to TiO_2 plays an important role in DSSC [14–17]. Zinc oxide materials have drawn the attention of researchers because of the wide band gap and its applications in electronics, photoelectronics and sensors [18]. The ZnO material possesses a wide band gap, low resistance and high light trapping characteristics that make it suitable for solar cells applications. The pure ZnO

*Corresponding author: tel: +919017447500,
e-mail: *amrik23kuk@gmail.com*

nanostructures show weak optical features that are result of point defects such as oxygen vacancies or interstitial Zn. Therefore, they cannot be used directly in the industry [19]. As a result, doping of ZnO with a convenient element can be used to modify optical and magnetic properties. Furthermore, in order to make optoelectronic devices, n-type and p-type states are needed [20–22]. The most commonly occurring lanthanide/transition metals are used as dopants. This is because these compounds have been widely used as high-performance luminescent devices, magnets, catalysts, and other functional materials. Many researchers have reported the influence of annealing temperature of doped ZnO film on the DSSCs performances [23]. Efficiency of the cell can also be improved by modifying the various parameters like thickness, porosity of semiconductor oxide photoanode and counterelectrode of DSSCs [24–26]. Sahu [27] reported the influences of dopant concentration and substrate temperature on the properties of the Ag-ZnO films. Duan *et al.* [28,29] reported the synthesis of Ag-ZnO films on Si substrates by DC reactive sputtering technique. The Ag doped ZnO films exhibit various optical and electrical properties that depend on the deposition temperature and silver content.

ZnO thin films can be synthesized by using different fabrication methods, including vapour phase processing approaches such as physical vapour deposition and chemical vapour deposition and wet solution processing approaches such as sol-gel process [30,31]. Different techniques result in different properties of ZnO thin films [32,33]. The sol-gel spin coating method has been widely adopted for the fabrication of transparent and conducting oxide due to its simplicity, safety, no need of costly vacuum system and applicability for large area coating. The sol-gel method also offers other advantages such as suitable surface morphology at low crystallizing temperature and the easy control of chemical components during sol-gel preparation [33,34]. Proper selection of concentration and nature of dopants in host materials like ZnO may improve the photon to electron conversion efficiency of DSSCs. Different types of dopants offer much broader range of possibilities that favour the performance of DSSCs. For a case, doping of such type of materials in ZnO photoanode may have possibility to open new avenues for unique optical, structural and electrical properties that could be helpful in research and industry related to renewable energy sources with broad application perspectives.

In the present work, silver doped ZnO thin films were deposited on ITO glass by sol-gel spin coating. The aim of this work was to produce p-type doping of ZnO film/ITO substrate to be used in practical applications. The deposited ZnO films on ITO substrate act as photoanodes for dye sensitized solar cells. Structure and optical properties have also been investigated for ZnO thin film samples. The photovoltaic performance of assembled solar cells was analysed.

II. Experimental

2.1. ZnO and Ag doped ZnO sol preparation

Zinc acetate dehydrate (Sigma Aldrich) and silver nitrate (Sigma Aldrich, 99.9%) were taken as ZnO and silver precursors, respectively. Firstly 5.949 g of zinc acetate dehydrate was added into 25 ml of ethanol and stirred for one hour at 60 °C and then monoethanolamine (Merck, 99% USA) was added into it. A clear and transparent ZnO sol was obtained after sometime and left at room temperature for 24 hours. Molar ratio of zinc acetate dihydrate and ethanolamine was maintained at 1 : 1 [33]. In addition to the pure ZnO, two doped ZnO sols with 0.5 and 1.5 mol% of silver were prepared by dissolving of appropriate amount of silver nitrate into acetonitrile (Sigma Aldrich 99.9%) and then added into stirred ZnO sol.

2.2. Photoanode preparation

Photoelectrode of ZnO and doped ZnO films were prepared by deposition of the obtained sols on ITO substrate via spin coating technique and scotch tape was used as a spacer. The speed of spin coater (MTI Corporation) was adjusted at 3000 rpm during one minute and then each film was dried on hot plate maintained at 180 °C for 10 minutes for removal of extra solvents. For desired thickness of films the steps of coating were performed three times and then the films were annealed at 550 °C for 1 h, with ramp rate of 10 °C/min. The thicknesses of films were obtained in the range of 310–330 nm.

For sensitization purposes, the as-fabricated photoelectrodes were dipped in dye solution (mixture of 0.5 mM of N719 dye and ethanol) for 24 hours and washed with ethanol for the removal of extra dye and then dried.

2.3. Counterlectrode preparation

For the preparation of platinum coated ITO/glass counterelectrode, the solution was made from 5 mM $PtCl_4$ (Sigma Aldrich, 99.9%) in isopropanol. The solution was poured on ITO glass substrate and spun for 1 min at 2800 rpm. The platinum films were dried at 130 °C for 15 minutes on the hot plate and then sintered at 400 °C for 15 minutes for removal of extra solvents [22]. Finally, the light grey coloured films were obtained.

2.4. Assembling of DSSCs

For the complete fabrication of DSSCs the dye sensitized photoelectrode and counterlectrode were combined together and an electrolyte solution was injected between the electrodes. Electrolyte solution (brown coloured) was made from 0.05 M lithium iodide (LiI Sigma Aldrich, 99.9%) and 0.5 mM iodine (I_2, Sigma Aldrich, 99.9%) in acetonitrile (Sigma Aldrich 99.9%) [22].

2.5. Characterization techniques

The XRD patterns of the prepared films were obtained by Rigaku Miniflex 600 diffractometer (using Cu-Kα, scan speed of 0.5–2°/min and λ = 1.541 Å). The crystallite size D was calculated using Scherrer formula [35]:

$$D = \frac{k \cdot \lambda}{\beta \cos\theta} \quad (1)$$

where β is the full width at half maximum of the diffraction 101 peak, λ is the X-ray wavelength and θ is the Bragg's angle. The SEM images of the samples were studied by JEOL scanning electron microscope (SEM JEOL) and UV-visible transmission spectra were recorded by UV-visible spectrometer set up (SHIMAZDU, UV 200–1000 nm). The photocurrent-voltage (J-V) characteristics of the assembled devices were measured using using AM-1.5 solar simulator (New Port Model, 96000) with xenon lamp (max. 150 W) and source meter (Keithley, Model 2400) at room temperature. Incident light intensity and active cell area were 100 mW/cm^2 (one sun illumination) and 1×1 cm, respectively. The thickness of the thin films was measured by Ellipsometer set up (Model No: HO-ED-P15, rotation range 70 degrees).

III. Results and discussion

3.1. Structural characterization

The crystallinity, crystallographic orientation and phase evaluation of the sol-gel spin coated ZnO films were examined by XRD measurements, as presented in Fig. 1. The XRD pattern confirms that ZnO has hexagonal wurtzite structure [28,29]. The main peaks of ZnO film correspond to the crystalline planes (100), (002), (101), (102) and (110) at angles of 32.68°, 35.34°, 36.68°, 48.16° and 57.32°, respectively. With 0.5 mol% doping of silver the peak corresponding to (101) plane shifted slightly to lower angle and again shifted to higher angle side at 1.5 mol% doping, which means that stress or strain were produced in the film. The intensity of XRD peak corresponding to plane (101) slightly degraded for the sample with 1.5 mol% of silver. From XRD analysis, the crystallite size corresponding to (101) plane of the pure and doped ZnO with 0.5 and 1.5 mol% silver were around 31, 30 and 25 nm, respectively. The slight degradation in peaks intensity found in the sample with 1.5 mol% of Ag is most likely due to the distortion in crystalline structure [36,37]. Structural parameters of the films are presented in Table 1.

Figures 2a, 2b and 2c show the SEM images of ZnO, ZnO:Ag0.5% and ZnO:Ag1.5%, respectively. The SEM image of the pure ZnO film shows that there is a uniform arrangement of grains. The average grain size of ZnO was measured as 44.5 nm. The surface of the ZnO film doped with 1.5 mol% Ag seems to be smooth, compared to other samples.

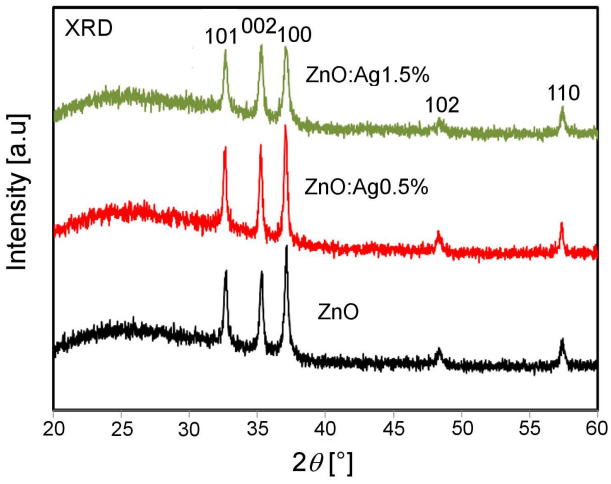

Figure 1. XRD pattern of silver doped ZnO films

Table 1. Structural parameters of ZnO films

Sample	FWHM [°]	Peak position [°]	Crystallite size [nm]
ZnO	0.2824	36.68	30.97
ZnO:Ag0.5%	0.2902	36.58	30.13
ZnO:Ag1.5%	0.3512	37.0	24.91

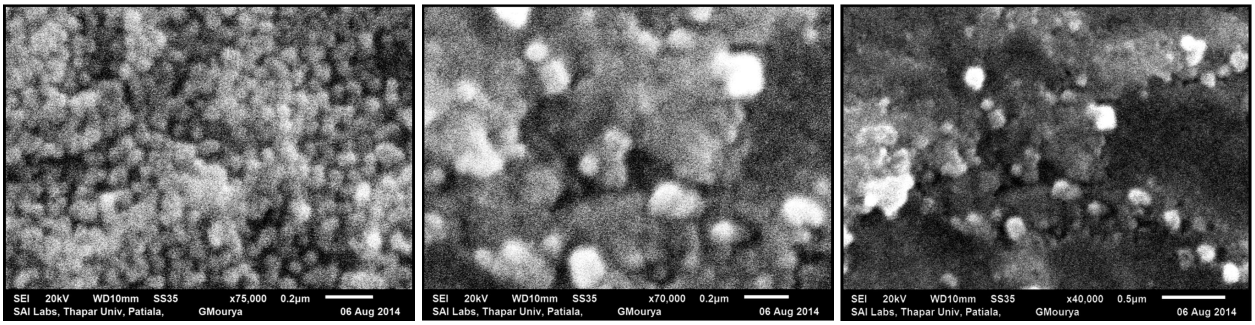

(a) (b) (c)

Figure 2. SEM images of a) pure ZnO film, b) ZnO:Ag0.5% and c) ZnO:Ag1.5%

3.2. Optical properties

Investigation of optical properties of the sol-gel spin coated ZnO thin films has been performed by UV-visible spectroscopy and the results are shown in Figs. 3 and 4. The absorbance of ZnO films is in the range of 6–30% in the visible portion of spectrum. The absorbance of the ZnO films slightly increases with addition of 0.5 mol% Ag and decreases with higher amount of silver (1.5 mol% Ag).

The transmission of the ZnO films was in the range of 65–90% in the portion of visible spectrum. With the increase in doping to 0.5 mol% of silver the transmission of the film slightly decreases and then it increases for the ZnO film with 1.5 mol% of silver. The slight decrease in transmittance was due to rough and porous surface of the film, while smooth surface of 1.5 mol% ZnO has increased the transmittance. Sutanto *et al.* have also reported similar types of results in the case of ZnO films [38]. Kim *et al.* also reported the behaviour of absorbance for doped ZnO films [39].

The band gap variations of ZnO-based films are shown in Fig. 5. The optical absorption data were analysed using the relation of optical absorption in semiconductor near band edge [40]:

$$\alpha \cdot h \cdot \nu = \left(h \cdot \nu - E_g\right)^n \qquad (2)$$

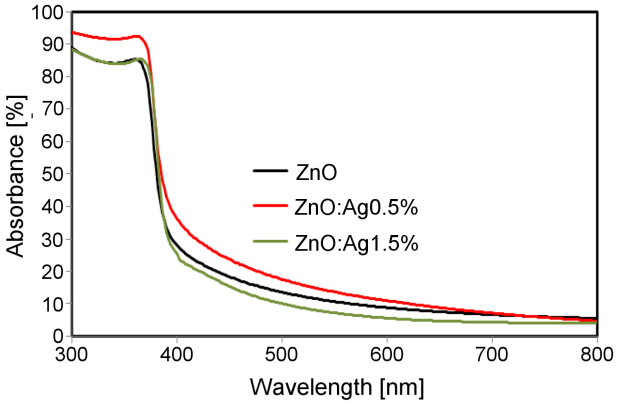

Figure 3. Absorbance spectra of doped ZnO films

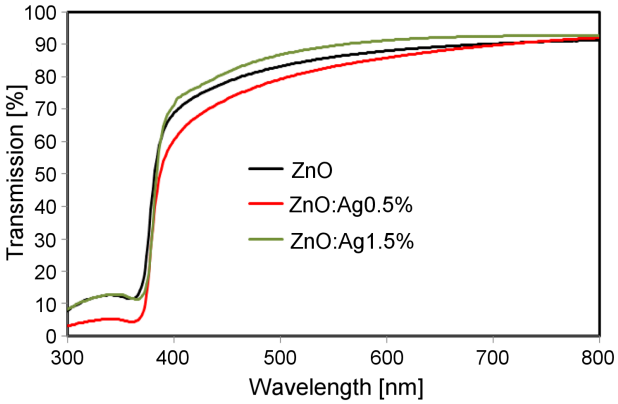

Figure 4. UV-visible transmission spectra of silver doped ZnO films

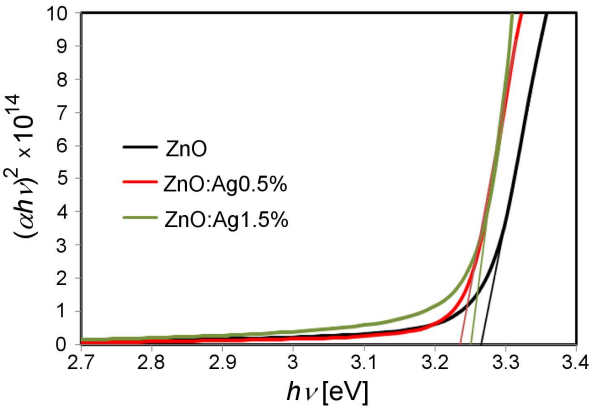

Figure 5. Band gap variations in silver doped ZnO films

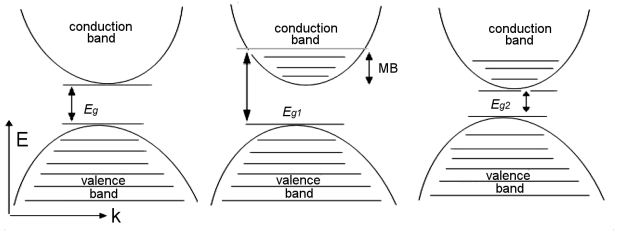

Figure 6. Variation of the band gap due to the Burstein-Moss shift [44]

where, E_g is the separation between bottom of the conduction band and top of the valence band, $h \cdot \nu$ is the photon energy and n is a constant. Value of n depends on the probability of transition; it takes values as ½ and 2 for direct allowed and indirect allowed, respectively. The band gap of the pure and ZnO films doped with 0.5 mol% and 1.5 mol% of silver are 3.269, 3.235 and 3.257 eV, respectively (Fig. 5). The narrowing of band gap with the addition of Ag is most likely due to the substitution of Ag^{2+} into the Zn^{2+}, according to the conclusions of similar study [41]. Presumably, Ag and O states are overlapped to form an impurity band, which shifts the Fermi level [42]. Silver doping in ZnO provides the impurity band in the energy gap, which could be due to the formation of the p-type in this substance. It should be mentioned that this reduction in energy gap led to the increased efficiency in the use of these materials in optoelectronic devices [43]. However, increase in the band gap of the material at high doping level has been reported due to the Burstein-Moss (MB) shift (Fig. 6) [44–46]. The Burstein-Moss shift in the material is the function of the carrier concentration.

Figure 7 shows the UV-visible absorbance of the N719 dye loaded ZnO (undoped and doped) films in the wavelength range of 300–800 nm. The main absorbance peaks are observed at wavelengths of 310, 350 and 538 nm. The absorbance of the dye loaded ZnO film with 0.5 mol% of silver is the highest as compared to other samples.

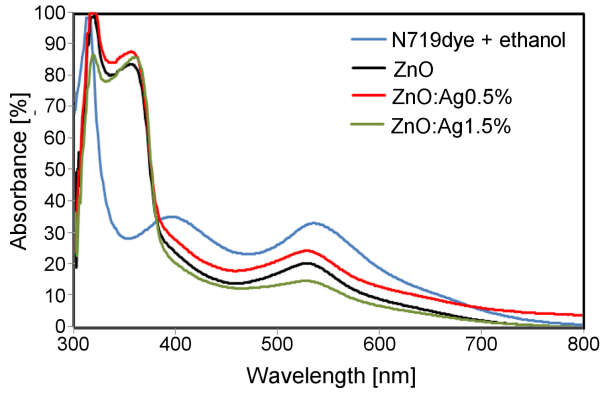

Figure 7. UV-visible absorption spectra of N719 dye ethanol solution and dye loaded undoped and doped ZnO films

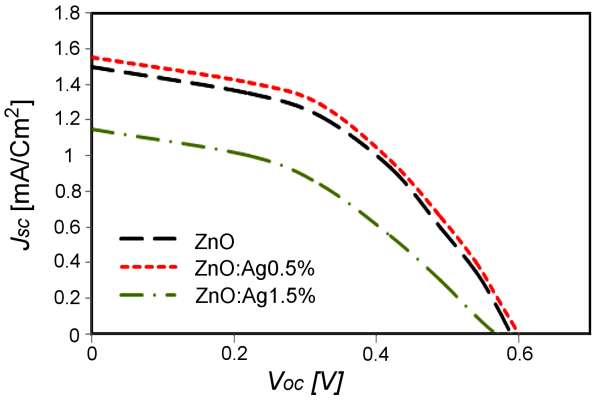

Figure 8. *J-V* characteristics of DSSCs

3.3. Photovoltaic performances of DSSCs

The values of fill factor (FF) and efficiency (η) of DSSC were calculated by following equations:

$$FF = \frac{I_m \cdot V_m}{I_{SC} \cdot V_{OC}} \tag{3}$$

$$\eta = \frac{I_{SC} \cdot V_{OC} \cdot FF}{P_{in}} \tag{4}$$

where V_{OC} is open circuit voltage, I_{SC} is short circuit voltage, I_m is maximal current, V_m maximal voltage and P_{in} is the input power provided to DSSC. The current-voltage characteristics of the fabricated DSSC are shown in the Fig. 8, while the relevant data extracted from the curves are presented in Table 2. The results of similar type of research work, reported by different researchers, are shown in Table 3.

The fill factor of ZnO, ZnO:Ag0.5% and ZnO:Ag1.5% is 0.47, 0.48 and 0.42, respectively. The current density was influenced by the dopants concentration. The calculated efficiency of the fabricated DSSCs with ZnO photoanode doped with 0, 0.5 and 1.5 mol% of silver are 0.42%, 0.44% and 0.27%, respectively. The DSSC based ZnO doped with 0.5 mol% of silver showed better photovoltaic performance. The amount of light absorbed by dye molecules increases scattering that leads to the large number of excited electrons and thus the highest performance was achieved for the film doped with 0.5 mol% of silver. The lower performance of the ZnO film doped with 1.5 mol% Ag is due to the degraded crystalline nature as compared to other samples.

IV. Conclusions

DSSCs were constructed with the pure ZnO and 0.5 and 1.5 mol% silver doped ZnO photoanodes, prepared by a simple sol-gel spin coating technique. The structural analysis confirmed that the prepared thin films consist of ZnO wurtzite phase. Further studies have also revealed that there was a change in the crystal structure that occurred with increasing doping concentration of silver. The structural observations indicate that Ag doped ZnO films have maintained the crystal structure at low doping concentration 0.5 mol%, but with 1.5 mol% doping it slightly degraded. The crystallite sizes, calculated from XRD data for 0, 0.5 and 1.5 mol% silver doped ZnO were obtained as 31, 30 and 25 nm, respectively. The transmission of ZnO film decreases at 0.5 mol% and again increases at 1.5 mol% of silver doping. The band gap values of the pure and ZnO films doped with 0.5 and 1.5 mol% of silver were measured as 3.269, 3.235 and 3.257 eV, respectively. The fill factor values obtained for ZnO, 0.5 mol% and 1.5 mol% silver doped ZnO were 0.47, 0.48 and 0.42, respectively. The calculated efficiencies of DSSCs based on the pure and ZnO films doped with 0.5 and 1.5 mol% of silver were 0.42, 0.44 and 0.27%, respectively. DSSC with ZnO film doped with 0.5 mol% Ag shows higher photovoltaic performance as compared to other samples.

Table 2. Photovoltaic parameters of DSSCs with different photoelectrodes

Sample	FF	V_{OS} [V]	J_{SC} [mA/cm^2]	Efficiency [%]
ZnO	0.47	0.59	1.50	0.42
ZnO:Ag0.5%	0.48	0.60	1.55	0.44
ZnO:Ag1.5%	0.42	0.57	1.15	0.27

Table 3. Comparison of performance parameters of DSSCs

V_{OC} [V]	J_{SC} [A·m/cm^2]	Efficiency [%]	References
0.374	0.9	0.13	[47]
0.574	2.08	0.56	[23]
0.460	2.2	0.29	[48]

Acknowledgements: Financial support from IUAC, New Delhi (India) and experimental support from SAI Labs, Thapar University, Patiala (India) are gratefully acknowledged.

References

1. B.O. Regan, M. Gratzel, "A low-cost, high-efficiency solar cell based on dye-sensitized colloidal TiO_2 films", *Nature*, **353** [6346] (1991) 737–740.
2. F.F. Ngaffo, A.P. Caricato, M. Fernandez, "Structural properties of single and multilayer ITO and TiO_2 films deposited by reactive pulsed laser ablation deposition technique", *Appl. Surf. Sci.*, **253** [1] (2007) 6508–6511.
3. M. Gratzel, "Conversion of sunlight to electric power by nanocrystalline dye sensitized solar cells", *Nature*, **164** (2004) 3–14.
4. M. Gratzel, "Photoelectrochemical cells", *Nature*, **414** [6861] (2001) 338–344.
5. R.S. Reddy, A. Sreedhar, A.S. Reddy, S. Uthanna, "Effect of film thickness on the structural morphological and optical properties of nanocrystalline ZnO films formed by RF magnetron sputtering", *Adv. Mat. Lett.*, **3** [3] (2002) 239–245.
6. J. Bisquert, D. Cahen, G. Hodes, S. Ruhle, A. Zaban, "Physical chemical principles of photovoltaic conversion with nanoparticulate, mesoporous dye-sensitized solar cells", *J. Phys. Chem. B*, **108** [24] (2004) 8106–8118.
7. T. Minami, J. Oda, J. Nomoto, "Effect of target properties on transparent conducting impurity-doped ZnO thin films deposited by DC magnetron sputtering", *Thin Solid Films*, **519** (2010) 385–390.
8. H. Chang, M.J. Kao, T.L. Chen, H.G. Kuo, K.C. Choand, X.P. Lin, "Natural sensitizer for dye-sensitized solar cell using three layers of photoelectrode thin films with a schottky barrier", *Am. J. Engg. Applied Sci.*, **4** (2011) 214–222.
9. C. Longo, M.A.D. Paoli, "Dye-sensitized solar cells: A successful combination of materials", *J. Braz. Chem. Soc.*, **14** [3] (2003) 889–901.
10. M. Gratzel, "Perspectives for dye-sensitized nanocrystalline solar cells", *Prog. Photovoltaics*, **8** (2000) 171–185.
11. J.W. Hoon, K.Y. Chan, J. Krishnasamy, T.Y. Tou, D. Knipp, "Direct current magnetron sputter-deposited ZnO thin films", *Appl. Surf. Sci.*, **25** [7] (2011) 2508–2515.
12. D. Jyoti, D. Mohan, A. Singh, D.S. Ahlawat, "A critical review on mesoporous photoanodes for dye-sensitized solar cells", *Mater. Sci. Forum*, **771** (2014) 53–69.
13. G. Franco, J. Gehring, L.M. Peter, E.A. Ponomarev, "Frequency-resolved optical detection of photoinjected electrons in dye-sensitized nanocrystalline photovoltaic cells", *J. Phys. Chem. B*, **103** [4] (1999) 692–698.
14. N.J. Cherepy, G.P. Smestad, M. Gratzel, Z.G. Zhang, "Ultrafast electron injection: Implications for a photoelectrochemical cell utilizing an anthocyanindye-sensitized TiO_2 nanocrystalline electrode", *J. Phys. Chem. B*, **101** (1997) 9342–9351.
15. L.M. Peter, K.G.U. Wijayantha, "Intensity dependence of the electron diffusion length in dye-sensitised nanocrystalline TiO_2 photovoltaic cells", *Electrochem. Comm.*, **1** [2] (1999) 576–580.
16. K. Fredin, J. Nissfolk, A. Hagfeldt, "Brownian dynamics simulations of electrons and ions in mesoporous films", *Sol. Energy Mater. Sol. Cells*, **86** [1-2] (2005) 283–297.
17. N.W. Duffy, L.M. Peter, R.M.G. Rajapakse, K.G.U. Wijayantha, "A novel charge extraction method for the study of electron transport and interfacial transfer in dye sensitised nanocrystalline solar cells", *Electrochem. Comm.*, **2** [9] (2000) 658–662.
18. A. Moezzi, A.M. McDonagh, M.B. Cortie, "Zinc oxide particles: Synthesis, properties and applications", *Chem. Eng. J.*, **185-186** (2012) 1–22.
19. M. Ahmad, J. Zhao, J. Iqbal, W. Miao, L. Xie, R. Mo, J. Zhu, "Conductivity enhancement by slight indium doping in ZnO nanowires for optoelectronic applications", *J. Phys. D: Applied Phys.*, **42** [16] (2009) 165406.
20. L.M. Peter, K.G.U. Wijayantha, "Electron transport and back reaction in dye sensitised nanocrystalline photovoltaic cells", *Electrochim. Acta*, **45** [28] (2000) 4543–4551.
21. C.P. Chen, M.Y. Ke, C.C. Liu, Y.J. Chang, F.H. Yang, J.J. Huang, "Observation of 394 nm electroluminescence from low-temperature sputtered n-ZnO/SiO_2 thin films on top of the p-GaN heterostructure", *Appl. Phys. Lett.*, **91** [9] (2007) 091107.
22. A. Singh , D. Mohan, D.S. Ahlawat, Richa, "Influence of dye loading time and electrolytes ratio on the performance spin coated ZnO photoanode based dye sensitized solar cells", *Orient. J. Chem.*, **32** [2] (2016) 1049–1054.
23. L. Roza, M.Y.A. Rahman, A.A. Umar, M.M. Salleh, "Boron doped ZnO films for dye-sensitized solar cell (DSSC): effect of annealing temperature", *J. Mater. Sci.: Mater. Electron.*, **27** [8] (2016) 8394–8401.
24. K. Hongsith, N. Hongsith, D. Wongratanaphisan, A. Gardchareon, S. Phadungdhitidhada, S. Choopun, "Efficiency enhancement of ZnO dye-sensitized solar cells by modifying photoelectrode and counterelectrode", *Energy Procedia*, **79** (2015) 360–365.
25. K. Radhamma, A.S. Reddy, S. Uthanna, "Structural, electrical and optical properties of molybdenum doped zinc oxide films formed by magnetron sputtering", *Adv. Mater. Lett.*, **6** [9] (2015) 834–839.
26. S.H. Lee, S.H. Han, H.S. Jung, H. Shin, J. Lee, "Al-doped ZnO thin film: A new transparent conducting layer for ZnO nanowire-based dye-sensitized solar cells", *Phys. Chem. C*, **114** [15] (2010) 7185–7189.
27. D.R. Sahu, "Studies on the properties of sputter deposited Ag-doped ZnO films", *Microelectr. J.*, **38** (2007) 1252–1256.
28. L. Duan, B. Lin, W. Zhang, S. Zhong, Z. Fu, "Enhancement of ultraviolet emissions from ZnO films by Ag doping", *Appl. Phys. Lett.*, **88** [23] (2006) 232110.
29. N.L. Tarwal, P.S. Patil, "Enhanced photoelectrochemical performance of Ag-ZnO thin films synthesized by spray pyrolysis technique", *Electrochim. Acta*, **56** (2011) 6510–6516.
30. L. Znaidi, "Sol-gel-deposited ZnO thin films: A review", *Mater. Sci. Eng. B*, **174** (2010) 18–30.
31. L. Wei, P. Xingping, L. Xueqin, H. Zhiwei, W. Yinyue, "Preparation and properties of ZnO thin films deposited by sol-gel technique", *Front. Mater. Sci.*, **1** [1] (2007) 88–91.
32. T. Sahoo, M. Kim, M.H. Lee, L.W. Jang, J.W. Jeon, J.S. Kwak, I.Y. Ko, I.H. Lee, "Nanocrystalline ZnO thin films by spin coating-pyrolysis method", *J. Alloys Compd.*, **491** [1] (2010) 308–313.
33. C. Thanachayanont, V. Yordsri, C. Boothroyd, "Mi-

crostructural investigation and SnO nanodefects in Spray-pyrolyzed SnO_2 thin films", *Mater. Lett.*, **65** [17] (2011) 2610–2613.
34. K. Okamura, B. Nasr, R.A. Brand, H. Hahn, "Solution-processed oxide semiconductor SnO in p-channel thin-film transistors", *J. Mater. Chem.*, **22** [11] (2012) 4607–4610.
35. P. Debye, "Scattering of X-rays", *Ann. Phys.*, **351** [6] (1915) 809–823.
36. K.H. Kim, K. Utashiro, Z. Jin, Y. Abe, M. Kawamura, "Dye sensitized solar cells with sol gel solution processed Ga doped ZnO passivation layer", *Int. J. Electrochem. Sci.*, **8** (2013) 5183–5190.
37. Y.Y. Çaglar, "Sol-gel derived nanostructure undoped and cobalt doped ZnO: Structural, optical and electrical studies", *J. Alloys Compd.*, **560** (2013) 181–188.
38. H. Sutanto, S. Wibowo, L. Nurhasanah, E. Hidayanto, H. Hadiyanto, "Ag doped ZnO thin films synthesized by spray coating technique for methylene blue photodegradation under UV irradiation", *Int. J. Chem. Eng.*, **2016** (2016) 6195326.
39. M.S. Kim, K.G. Yim, S. Kim, G. Nam, D.Y. Lee, J.S. Kim, J.Y. Leem, "Growth and characterization of Indium-doped zinc oxide thin films prepared by sol-gel method", *Acta Phys. Polonica A*, **121** (2012) 217–220.
40. J.I. Pankove, *Optical Processes in Semiconductors*, Dover, New York, 1971.
41. S.H. Jeong, B.N. Park, S.B. Lee, J.H. Boo, "Metal-doped ZnO thin films: Synthesis and characterizations", *Surf. Coat. Tech.*, **201** (2007) 5318–5322.
42. M. Thomas, W. Sun, J. Cui, "Mechanism of Ag doping in ZnO nanowires by electrodeposition: Experimental and theoretical insights", *J. Phys. Chem. C*, **116** [10] (2012) 6383–6391.
43. S.P. Lim, A. Pandikumar, H. N. Lim, R. Ramaraj, N.M. Huangc, "Boosting photovoltaic performance of dye-sensitized solar cells using silver nanoparticle-decorated N,S-co-doped-TiO_2 photoanode", *Sci. Reports*, **5** (2015) 1–12.
44. T.S. Moss, *Optical Properties of Semiconductor*, Butterworths Sci. Pub. Ltd, London, 1959.
45. N. Yoshii, A. Nakamura, S. Hosaka, "Controlled structure of zinc oxide by means of side flow type MOCVD", *ECS Transactions*, **16** [12] (2008) 3–11.
46. C. Bauer, G. Boschloo, E. Mukhta, A. Hagfeldt, "Electron injection and recombination in $Ru(dcbpy)_2(NCS)_2$ sensitized nanostructured ZnO", *J. Phys. Chem. B*, **105** [24] (2001) 5585–5588.
47. M.F. Hossain, S. Biswas, M. Shahjahan, T. Takahashi, "Study of sol-gel derived porous ZnO photoelectrode for the application of dye-sensitized solar cells", *J. Vac. Sci. Technol.*, **27** (2009) 1047–1051.
48. A. Apostolopoulou, D. Karageorgopoulos, A. Rapsomanikis, A. Stathatos, "Dye-sensitized solar cells with zinc oxide nanostructured films made with amine oligomers as organic templates and gel electrolytes", *J. Clean Energy Technol.*, **4** [5] (2016) 311–315.